Complex impedance studies on tungsten-bronze electroceramic: $Pb_2Bi_3LaTi_5O_{18}$

C. K. SUMAN, K. PRASAD*, R. N. P. CHOUDHARY†
University Department of Physics, T. M. Bhagalpur University, Bhagalpur 812 007, India
E-mail: k_prasad65@yahoo.co.in

Published online: 17 January 2006

Complex impedance analysis of polycrystalline $Pb_2Bi_3LaTi_5O_{18}$, prepared by a high-temperature solid-state reaction technique has been carried out. XRD analysis indicated the formation of a single-phase orthorhombic structure. Impedance plots were used as a tool to analyse the behaviour of the sample as a function of frequency and temperature. The bulk resistance has been observed to decrease with rise in temperature showing a typical negative temperature coefficient of resistance (NTCR) type behaviour like that of semiconductors. The ac impedance studies revealed the presence of grain boundary effect at 450°C and showed polydispersive non Debye-type dielectric relaxation. The frequency dependent ac conductivity at different temperatures indicated that the conduction process is thermally activated process. The activation energy for bulk (0.67 eV) and grain boundary (0.73 eV) was estimated from the temperature variation of respective conductivities.

1. Introduction

Among ferroelectric materials of different structural families (e.g. perovskite, tungsten-bronze, layered, etc.) available now a days, some rare-earth based compounds of tungsten-bronze (TB) family such as $(Sr,Ba)Nb_2O_6$ [1–6], $(Pb,Ba)Nb_2O_6$ [3, 7], $Pb_2Bi_4Ti_5O_{18}$ [8], $(Pb,K)LiTa_{10}O_{30}$ [9], $Ba_2NaNb_5O_{15}$ [10], $Ba_2Na_3RNb_{10}O_{30}$ (R = rare-earth ions) [11], $Ba_5RTi_3Nb_7O_{30}$ (R = Dy, Sm) [12], (R = Nd, Eu, Gd) [13], $Ba_4R_2Ti_4Nb_6O_{30}$ (R = Y, Sm, Dy) [14], $Ba_5Nd(Ti,Zr)Nb_7O_{30}$ [15], $Ba_{6-x}La_xNb_{10}O_{30+\delta}$ [16], $Pb_2Bi_3DyTi_5O_{18}$ [17], $(Ba_{1-x}\text{-}Sr_x)_2NaNb_5O_{15}$ [18], etc. have been found attractive because of their promising physical properties suitable for the fabrication of various electronic devices for industrial applications. The crystal structure of this family is based on the framework of corner sharing of distorted BO_6-octahedra in such a way that three different types of interstitial sites (A, B, C) are available for cation substitutions [19, 20]. Substitution of proper cations at these sites led to the enhancement of various physical properties required for the device applications such as electro-optic modulator, nonlinear optical devices, pyroelectric sensors, acousto-optic devices, etc. [9, 18, 21–25].

Continuous attempts have been made to investigate $Pb_2B_3RTi_5O_{18}$ (B ≡ Sb or Bi; R ≡ rare-earth ions) compounds with desired characteristics both from theoretical as well as application points of view. Recent studies on the electrical properties of $Pb_2Bi_3DyTi_5O_{18}$, $Pb_2Bi_3NdTi_5O_{18}$, $Pb_2Bi_3GdTi_5O_{18}$, $Pb_2Sb_3DyTi_5O_{18}$, and $Pb_2Sb_3LaTi_5O_{18}$ ceramics showed the presence of diffuse phase transition with low dielectric constant [17, 25–28]. The electrical properties in electroceramics are generally due to the contribution of various components and process such as intragrain, intergrain and electrode/interface processes. The charge transport can be due to the charge displacement, dipole reorientation and space charge formation. These charge transport process causes a number of different polarization mechanism that results frequency dispersion or dielectric relaxation in the materials under an ac field. The present work is an attempt to study the role of grain and grain boundaries on the electrical behaviour of $Pb_2Bi_3LaTi_5O_{18}$ (PBLT) and their dependence on temperature and frequency.

2. Theoretical background

Complex impedance spectroscopy is a promising nondestructive testing method for analyzing the electrical processes occurring in a compound on the application of small ac signal as input perturbation. The output response

*Author to whom all correspondence should be addressed.
†*Present Address*: Department of Physics & Meteorology, Indian Institute of Technology, Kharagpur 721302, India.
0022-2461
DOI: 10.1007/s10853-005-2620-5

of polycrystalline compound, when plotted in a complex plane plot represents grain, grain boundary and interface properties with different time constants leading to three successive semicircles. The frequency dependence of electrical data is interrelated to each other as

$$\left.\begin{aligned} \text{complex impedance, } Z^*(\omega) &= Z' - jZ'' \\ &= R_s - j/\omega C_s \\ \text{complex admittance, } Y^*(\omega) &= Y' + jY'' \\ &= 1/R_p + j\omega C_p \\ \text{complex permittivity, } \varepsilon^*(\omega) &= \varepsilon' - j\varepsilon'' \quad \text{and} \\ \text{complex modulus, } M^*(\omega) &= M' + jM''. \end{aligned}\right\} \quad (1)$$

These formalisms are interrelated as $M^* = 1/\varepsilon^* = j\omega C_o Z^* = j\omega C_o(1/Y^*)$ and the loss tangent, $\tan\delta = Z'/Z'' = \varepsilon''/\varepsilon' = M''/M'$, where R_s, C_s are the series resistance and capacitance; R_p, C_p are the parallel resistance and capacitance. The grain effect is shown by the appearance of a high frequency semicircle and second and third semicircles respectively represent grain boundary and electrode/interface contributions in the complex impedance plot. Therefore, the electrical conductivity due to these components (bulk, grain boundary and/or interface effects) can be represented as

$$\sigma_x = \frac{l}{R_\chi A} \quad (2)$$

where l and A are the thickness and area respectively and the suffix $x \equiv b$, gb or el indicate respectively the bulk, grain boundary or interface. The end point of each semicircle cuts real (Z')-axis in the complex impedance plot, giving rise to the respective value of resistance (e.g. R_b, R_{gb} or R_{el}). The semicircles in the impedance spectrum have a characteristic peak occurring at a unique relaxation frequency ($\omega_{\max} = 1/2\,\pi\, f_{\max}$) that indicates the electrical phenomena due to different components in the sample. It is expressed as $\omega_{\max} RC = \omega_{\max}\tau = 1$. Therefore,

$$f_{\max} = 1/(2\pi\tau) = 1/(2\pi RC) \quad (3)$$

The parameters such as relaxation frequency, relaxation time depends only on intrinsic properties of the material. These intrinsic properties gives rise to the distribution of resisitive and capacitive components in the materials on which relaxation time depends.

3. Experimental

A mixed high temperature solid-state reaction oxide method was used for the preparation of $Pb_2Bi_3LaTi_5O_{18}$ (PBLT) ceramic:

$$2PbO + \frac{3}{2}Bi_2O_3 + \frac{1}{2}La_2O_3 + 5TiO_2 \xrightarrow{\Delta} Pb_2Bi_3LaTi_5O_{18}$$

The initial AR-grade powders of PbO, Bi_2O_3, La_2O_3 and TiO_2 were taken in stoichiometric ratio. They were ground and heated at 1050°C for 10 h in air atmosphere. Two percent extra PbO was added to compensate lead loss. The calcined powder was then grounded and put in form of disks (10 mm diameter and 2 mm thickness). The optimized sintering conditions were 1090°C for 6 h in a closed medium. Completion of the reaction and the formation of the desired compound were checked by X-ray diffraction technique. The XRD spectra were taken on calcined powders of PBLT at room temperature using Cu K_α radiation ($\lambda = 0.15418$ nm) over a wide range of Bragg angles ($20° \le 2\theta \le 80°$) with a scanning speed $2°\ \text{min}^{-1}$. The surface morphology/microstructural study of the specimen has been carried out using a computer-controlled scanning electron microscope (SEM) (JEOL-JSM, Model: 5800F). The pellet was gold coated prior to being scanned under a high-resolution field emission gun scanning electron microscope. The electrical measurements were carried out on a symmetrical cell of type Ag|PBLT|Ag, where Ag is a conductive paint coated on either side of the pellet. Electrical impedance (Z), phase angle (θ), loss tangent and capacitance (C) were measured as a function of frequency (0.1 kHz–1 MHz) at different temperatures (20–500°C) using a computer-controlled LCR Hi-Tester (HIOKI 3532-50, Japan).

4. Results and discussion

4.1. Structure and microstructure analysis

A standard computer program (PowdMult) has been utilized for the XRD-profile (Fig. 1) fitting. Good agreement between the observed and calculated interplaner spacing (d-values) and no trace of any extra peaks due to constituent oxides, were found, suggesting that the compound is having a single-phase orthorhombic structure. The lattice parameters were estimated to be: $a = 8.332(1)$ Å, $b = 8.340(7)$ Åand $c = 9.778(2)$ Åwith an estimated error of $\pm 10^{-3}$ Å. The criterion adopted for evaluating the rightness, reliability of the indexing and the structure of PBLT was the sum of differences in observed and calculated d-values [i.e.

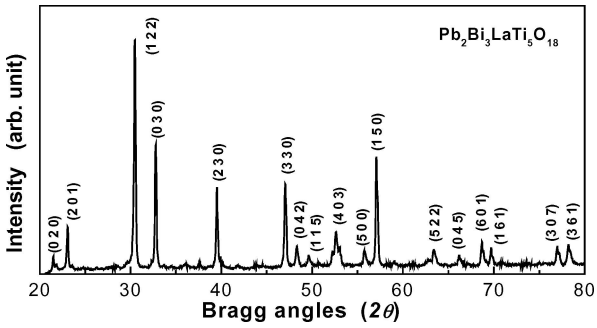

Figure 1 X-ray diffraction pattern of $Pb_2Bi_3LaTi_5O_{18}$ at room temperature.

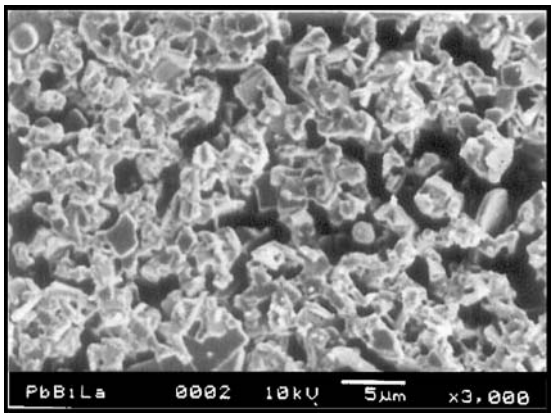

Figure 2 SEM micrograph of $Pb_2Bi_3LaTi_5O_{18}$ at 5 μm.

$\sum \Delta d = \sum (d_{obs} - d_{calc})]$ found to be minimum. The unit cell volume ($a \times b \times c$) was calculated to be 679.54 Å^3.

The SEM micrograph of sintered pellet is shown in Fig. 2. Grain shapes (almost spherical) are clearly visible indicating the existence of polycrystalline microstructure. The grain of unequal sizes (~2–3 μm) appears to be distributed homogeneously through out the sample. The presence of few voids of irregular dimension indicates that the sample has certain degree of porosity.

4.2. Impedance analysis

Fig. 3 shows the variation of the real part of impedance (Z') with frequency at different temperature (425 to 500°C). Also, inset figure shows the same between 25 to 400°C. It is observed that the magnitude of Z' decreases with the increase in both frequency as well as temperature. The Z' values for all temperatures merge above 100 kHz. This may be due to the release of space charges. It has been observed that in low temperature region the magnitude of Z' decreases with the rise in temperature i.e. showing negative temperature coefficient of resistance (NTCR) type behaviour as that of semiconductors. The curves also display single relaxation process and indicate increase in ac conductivity with the increase in temperature and frequency.

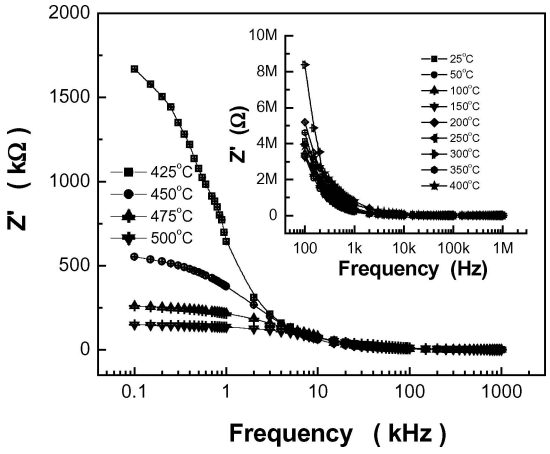

Figure 3 Variation of real part of impedance of $Pb_2Bi_3LaTi_5O_{18}$ with frequency at different temperature. Inset figure: Variation of real part of impedance up to 400°C.

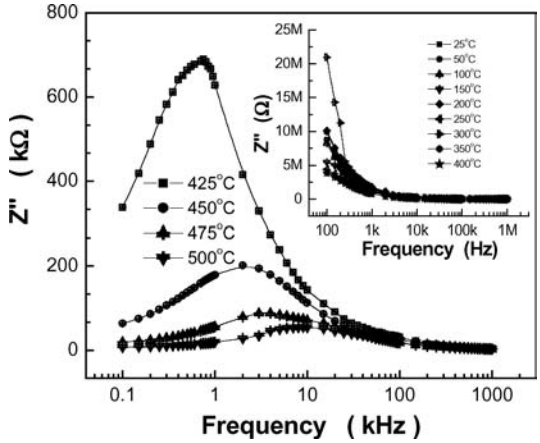

Figure 4 Variation of imaginary part of impedance of $Pb_2Bi_3LaTi_5O_{18}$ with frequency at different temperature. Inset figure: Variation of imaginary part of impedance up to 400°C.

Fig. 4 shows the variation of the imaginary part of impedance (Z'') with frequency at different temperature (425 to 500°C). The plots show that the Z'' values reach a maxima peak (Z''_{max}) for temperatures ≥400°C. For the temperature below 425°C, the peak was beyond the range of frequency measurement (Inset Fig. 4) and the value of Z''_{max} shifts to higher frequencies with increasing temperature indicating the increase in loss in the sample. The broadening in the peaks indicates a temperature dependent electrical relaxation phenomenon in the material. The peak heights are proportional to bulk resistance (R_b) according to equation [29]: $Z'' = R_b[\omega\tau/(1 + \omega^2\tau^2)]$ in Z'' versus frequency plots.

Fig. 5 shows the normalized imaginary parts of the impedance (Z''/Z''_{max}) as a function of frequency for PBLT at several temperatures. It seems that high temperature triggers another relaxation process. The Z''/Z''_{max}

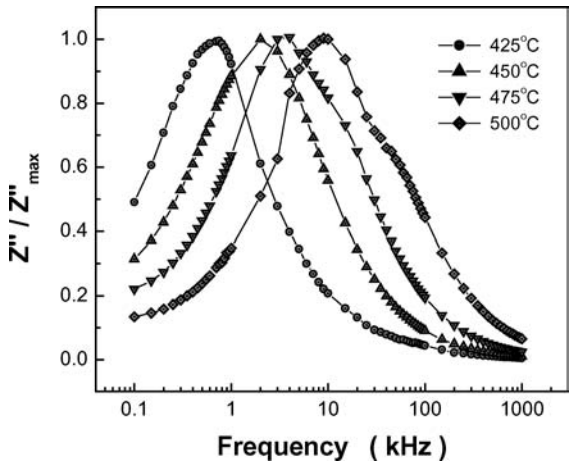

Figure 5 Normalized imaginary part of impedance (Z''/Z''_{max}) as a function of frequency for $Pb_2Bi_3LaTi_5O_{18}$ at several temperatures.

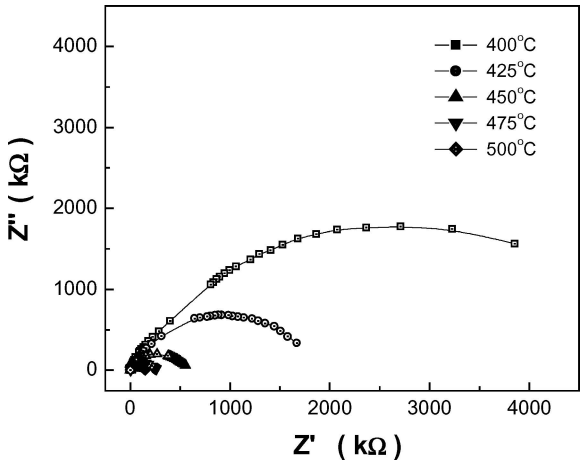

Figure 6 Nyquist diagram for $Pb_2Bi_3LaTi_5O_{18}$ at different temperature.

parameter exhibits a peak with a slightly asymmetric degree at each temperature especially at higher temperatures. The asymmetric broadening of the peaks suggests the presence of electrical processes in the material with a spread of relaxation time. The relaxation species in the material may possibly be immobile species/electrons at low temperatures and defects/vacancies at higher temperatures. The value of f_{max} shifts to higher side with increasing temperature indicating the increasing loss in the sample.

Fig. 6 shows a set of impedance data taken over a wide frequency range (100 Hz–1 MHz) at several temperatures as a Nyquist diagram. It is observed that with the increase in temperature the slope of the lines decreases and they bent towards real (Z') axis above 350°C and a semicircle could be traced, indicating the increase in conductivity of the sample. Above 425°C two semicircles could be obtained with different values of resistance for grain and grain boundary. Hence grain and grain boundary effects could be separated at these temperatures. This result successfully explains the presence of grain boundaries in PBLT, which is in consistent with the SEM (Fig. 2) where grains are well separated by the grain boundaries. Assuming series association of resistance and capacitance contribution for grain, grain boundary and electrode/interface behaviour, the solution for real and imaginary part of impedance can be formulated as

$$Z' = R_b/[1+(\omega/\omega_b)^2] + R_{gb}/[1+(\omega/\omega_{gb})^2] + R_{el}/[1+(\omega/\omega_{el})^2] \quad (4)$$

$$Z'' = R_b(\omega/\omega_b)/[1+(\omega/\omega_b)^2] + R_{gb}(\omega/\omega_{gb})/ \times [1+(\omega/\omega_{gb})^2] + R_{el}(\omega/\omega_{el})/ \times [1+(\omega/\omega_{el})^2] \quad (5)$$

These compounds are expected to loose traces of oxygen during sintering at high temperature as per the reaction (Kröger and Vink [30]):

$$O_o \rightarrow \frac{1}{2}O_2 \uparrow + V_o^{\bullet\bullet} + 2e^- \quad (6)$$

These defects affect impedance and capacitance in the formation of barrier layers at the grain-grain boundary interface [31]. During cooling of the samples after sintering reoxidation takes place. This oxidation is limited to surface and grain boundaries only due to insufficient time. The difference between resistance of grain boundary and grain, gives rise to barrier [31]. A third semicircle could also be seen above 475°C (Fig. 7), which could be due to the electrode effect. This type of electrical phenomenon is successfully explained by a brick layer model [32] considering an equivalent electrical circuit of a series of parallel combination of resistance and capacitance. It can also be observed that the peak maxima of the plots decrease with increasing temperature and the frequency for the maximum shifts to higher values with the increase in temperature. The appropriate equivalent circuit representation for PBLT at these temperatures, are shown in the inset of Fig. 7. The resistance of bulk (R_b), grain boundary

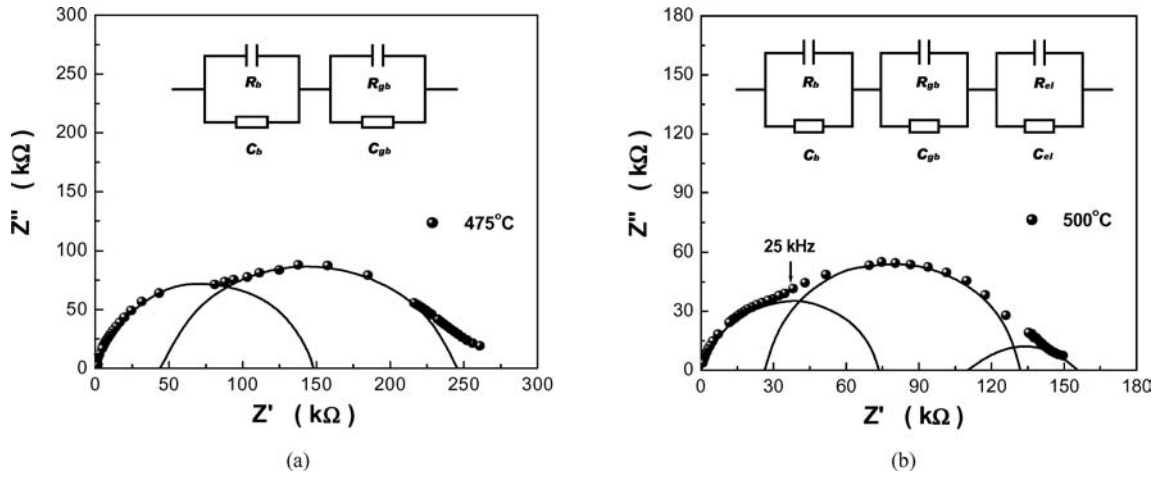

Figure 7 Complex impedance plots of $Pb_2Bi_3LaTi_5O_{18}$ at 475 and 500°C. Inset figure: Appropriate equivalent electrical circuit.

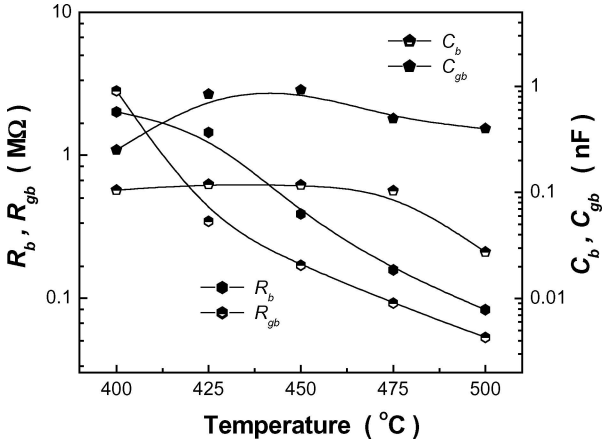

Figure 8 Variation of R_b, R_{gb}, C_b and C_{gb} with temperature for $Pb_2Bi_3LaTi_5O_{18}$.

(R_{gb}) and due to electrode effect (R_{el}) could directly be obtained from the intercept on the Z'-axis. The capacitances (C_b, C_{gb} and C_{el}) due to these effects can be calculated using the relation (3). The value of ω, the angular frequency can be estimated at the maxima of the semicircle for the component. The value of R_b, R_{gb}, R_{el}, C_b, C_{gb} and C_{el} at different temperature obtained from Cole-Cole plots at different temperatures is shown in Fig. 8. It can be seen that the values of R_b, R_{gb} and C_b decrease while the value of C_{gb} increases with the increment in temperature and at 500°C it decreases. The decrease in C_{gb} may be due to the introduction of material/interface effect (Fig. 8). The decrease in R_b with the rise of temperature indicates the NTCR behaviour of PBLT, which was also observed in Z'-frequency plot (Fig. 3). The relaxation times (τ) were estimated from the maxima of the semicircle due to bulk as well as grain boundary effects in the complex impedance plots (Fig. 7). The temperature variation of relaxation times due to bulk and grain boundary effects (Fig. 9) follows the Arrhenius relationship:

$$\tau = \tau_o \exp(-E_\tau / k_B T) \tag{7}$$

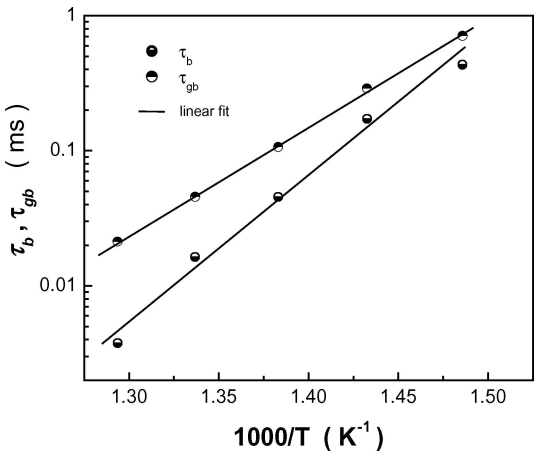

Figure 9 Temperature dependence of bulk and grain boundary relaxation times for $Pb_2Bi_3LaTi_5O_{18}$.

where τ_o is the pre-exponential factor. The activation energy, E_τ calculated from linear least squares fit to log τ_m–1/T data is 0.91 and 0.69 eV respectively for bulk and grain boundary.

Complex impedance formalism also provides information about the nature of dielectric relaxation. For pure monodispersive Debye process, one expects semicircular plots with the center located on the Z'-axis whereas, for polydispersive relaxation, these argand plane plots are close to circular arcs with end-points on the axis of reals and the center below this axis. The complex impedance in such situations is known to be described by Cole-Cole formalism [33]:

$$Z^*(\omega) = Z' + iZ'' = R\big/\left[1 + (i\omega/\omega_o)^{1-\alpha}\right] \tag{8}$$

where α represents the magnitude of the departure of the electrical response from an ideal condition and this can be determined from the location of the center of the Cole-Cole circles. When α goes to zero (1–$\alpha \rightarrow 1$) the Equation 3 gives rise to classical Debye's formalism. Fig. 7 depicts two representative plots for $T = 475$ and 500°C. It can be seen from these plots that the data is not represented by full semicircle (i.e. semicircle not centered on the abscissa axis, $\alpha > 0$), suggests that the dielectric relaxation to be of polydispersive non-Debye type. This may happen due to the presence of distributed elements in the material-electrode system [6] that results in the deviation from the pure semicircle in complex impedance plots.

4.3. Conductivity analysis

Fig. 10 shows the electrical conductivity $\sigma(\omega)$ of PBLT as a function of frequency at different temperature. The conductivity depends on frequency according to the 'universal dynamic response' for ionic conductors [34] given by the phenomenological law:

$$\sigma(\omega) = \sigma(0) + K \cdot \omega^n \tag{9}$$

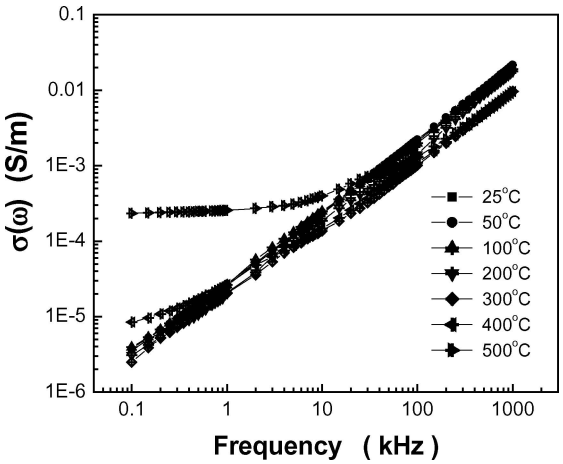

Figure 10 Variation of ac conductivity with frequency at different temperature for $Pb_2Bi_3LaTi_5O_{18}$.

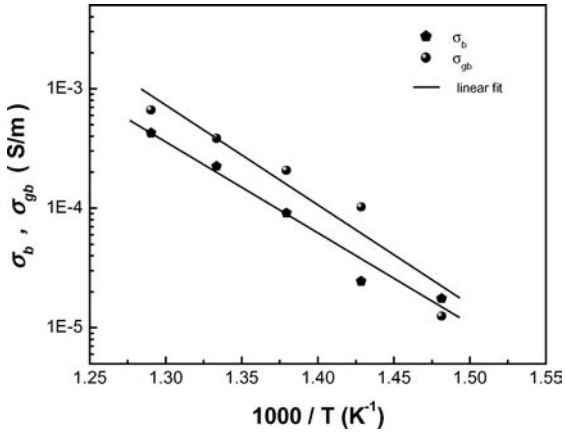

Figure 11 Variation of bulk and grain boundary conductivity with temperature for $Pb_2Bi_3LaTi_5O_{18}$.

where K is a thermally activated quantity and n is the frequency exponent and can takes the value less than 1. This indicates that the conduction process is a thermally activated process. It is observed that variation of $\sigma(\omega)$ with frequency show flattening with increment in temperature ($\geq$450°C). The switch from the frequency-independent $\sigma(0)$ to the dependent $\sigma(\omega)$ regions shows the onset of the conductivity relaxation phenomenon and the translation from long range hopping to the short range ion motion [34]. The dispersion in conductivity at low frequencies may be due to the electrode polarization. Also, it is observed that the electrical conductivity increases with the increase in temperature. A similar behaviour was observed in $Pb_2Sb_3LaTi_5O_{18}$ [28].

Fig. 11 shows the variation of bulk and grain boundary conductivities, obtained from the impedance data (Equation 2) against $10^3/T$. The nature of variation is almost linear over a wide temperature region obeys the Arrhenius relationship:

$$\sigma_x = \sigma_o \exp(-E_a/k_B T) \tag{10}$$

where E_a is the activation energy of conduction and T is the absolute temperature. The linear least squares fitting to the data at higher temperature region gives the values of $E_a = 0.67$ and 0.73 eV respectively for bulk and grain boundary. The low value of activation energy obtained could be attributed to the influence of electronic contribution to the conductivity. This value is comparable to other TB-type ferroelectric oxides [17, 25–28]. The increase in conductivity with temperature may be considered on the basis that within the bulk, the oxygen vacancies due to the loss of oxygen are usually created during sintering and the charge compensation follows Equation 6, which may leave behind free electrons making them n-type. The value of R^2 (regression coefficient indicating goodness of fit) for all the fittings, quoted in this paper, is excess of 0.995.

5. Conclusion

It is concluded that PBLT has orthorhombic structure at room temperature, the morphological features have been found to be in agreement with the XRD observation. Impedance analyses indicated the NTCR behaviour of PBLT and the presence of grain, grain boundary (400°C) and electrode (475°C) effects. Therefore, the electrical transport governed by grain boundary and/or electrode effect at these temperatures. The relaxation frequency shifted to higher frequencies with the increase of temperature. Complex impedance analysis suggested dielectric relaxation to be of polydispersive non-Debye type. The ac conductivity obeys the universal power law and the dispersion in conductivity was observed in the lower frequency region. Also, the frequency dependent ac conductivity at different temperatures indicated that the conduction process is thermally activated process. The activation energy for bulk and grain boundary was found respectively to be 0.67 and 0.73 eV.

Acknowledgment

One of us (KP) gratefully acknowledges Indian National Science Academy (INSA), New Delhi for providing visiting fellowship.

References

1. A. M. GLASS, *J. Appl. Phys.* **40** (1981) 4699.
2. W. W. HO, W. F. HALL, R. R. NEURGAONKAR, R. E. DEWAMES and T. L. MIM, *Ferroelectrics* **38** (1981) 833.
3. J. M. PÓVA, E. N. MOREIRA, D. GARCIA, D. U. P. SPÍNOLA, C. G. V. DO CARMO and J. A. EIRAS, *J. Kor. Phys. Soc.* **32** (1998) S1046.
4. C. ELISSALDE and J. RAVEZ, *ibid.* **32** (1998) S1022.
5. K. KAKIMOTO, H. KAKEMOTO, A. BABA, S. FUJITA and Y. MASUDA, *J. Euro. Ceram. Soc.* **21** (2001) 1569.
6. K. NAGATA, Y. YAMAMOTO, H. IGARASHI and K. OKAZAKI, *Ferroelectrics* **38** (1981) 853.
7. M. H. FRANCOMBE, *Acta. Cryst.* **13** (1960) 131.
8. M. E. LINES and A. M. GLASS, in "Principle and Applications of Ferroelectric and Related Materials" (Clarenden Press, Oxford, 1977).
9. V. HORNEBECQ, C. ELISSALDE, V. POROKHONSKYY, V. BOVTUN, J. PETZELT, I. GREGARA, M. MAGLIONE and J. RAVEZ, *J. Phys. Chem. Solids* **64** (2003) 471.
10. A. KEITSIRO, *J. Phys. Soc. Jpn.* **41**(3) (1976) 880.
11. K. S. SINGH, R. SATI and R. N. P. CHOUDHARY, *J. Mater. Sci. Lett.* **11** (1992) 788.
12. S. R. SHANNIGRAHI, R. N. P. CHOUDHARY, ATUL KUMAR and H. N. ACHARYA, *J. Phys. Chem. Solids* **59** (1998) 737.
13. R. N. P. CHOUDHARY, S. R. SHANNIGRAHI and A. K. SINGH, *Bull. Mater. Sci.* **6** (1999) 975.
14. R. PALAI, R. N. P. CHOUDHARY and H. S. TEWARI, *J. Phys. Chem. Solids* **62** (2001) 695.
15. A. PANIGRAHI, N. K. SINGH and R. N. P. CHOUDHARY, *ibid.* **63** (2002) 213.
16. Y. K. HWANG and Y. U. KWON, *Mater. Res. Bull.* **32** (1997) 1495.
17. C. K. SUMAN, K. PRASAD and R. N. P. CHOUDHARY, *Phys. Stat. Sol. (a)* **201** (2004) 3166.
18. K. S. RAO, T. N. V. K. V. PRASAD, A. S. V. SUBRAHMANYAM, J. H. LEE, J. J. KIM and S. H. CHO, *Mater. Sci. Engg.* **B98** (2003) 279.

19. C. J. RAWAN, *J. Mater. Res.* **13** (1998) 187.
20. P. B. JAMIESON, S. C. ABRAHAM and J. L. BERNSTEIN, *J. Chem. Phys.* **48** (1965) 5048.
21. R. R. NEURGAONKAR, W. KCORY, W. W. HO and W. F. HALL, *Ferroelectrics* **38** (1981) 857.
22. K. MEGUMI, N. NAGATSUMA, Y. KASHIWADA and Y. FURUHATA, *J. Mater. Sci.* **11** (1976) 1583.
23. J. C. TOLEDANO, *Phys. Rev. B* **12** (1975) 943.
24. R. R. NEURGAONKAR and W. K. CORY, *J. Opt. Soc. Am.* **3** (1986) 274.
25. C. K. SUMAN, K. PRASAD and R. N. P. CHOUDHARY, *Mater. Chem. Phys.* **82** (2003) 140.
26. *Idem.*, *Ind. J. Phys.* **78** (2004) 855.
27. C. K. SUMAN, K. PRASAD, S. N. CHOUDHARY and R. N. P. CHOUDHARY, *ibid.* **78** (2004) 849.
28. C. K. SUMAN, K. PRASAD and R. N. P. CHOUDHARY, *Bull. Mater. Sci.* **27** (2004) 547.
29. R. VON HIPPLE, in "Dielectrics and Waves" (John Wiley and Sons, NY, 1954).
30. F. A. KRÖGER and H. J. VINK, *Solid State Phys.* **3** (1956) 307.
31. R. C. DA and Y. G. YAN, *Electr. Elem. Mater.* **1** (1982) 25.
32. J. R. MACDONALD (Ed.), "Impedance Spectroscopy Emphasizing Solid Materials and Systems" (John Wiley and Sons, NY, 1987).
33. K. S. COLE and R. H. COLE, *J. Chem. Phys.* **9** (1941) 341.
34. J. GRIGAS, in "Microwave Dielectric Spectroscopy of Ferroelectrics and Related Materials" (Gordon and Breach Pub. Inc., Amsterdam, 1996).
35. R. MIZARAS, M. TAKASHIGE, J. BANYS, S. KOJIMA, J. GRIGAS, S.-I. HAMAZAKI and A. BRILINGAS, *J. Phys. Soc. Jpn.* **66** (1997) 2881.

Received 25 February
and accepted 27 May 2005